2010

Diverse voltage-sensitive dyes modulate GABAA receptor function

Steven Mennerick
Washington University School of Medicine in St. Louis

Mariangela Chisari
Washington University School of Medicine in St. Louis

Hong-Jin Shu
Washington University School of Medicine in St. Louis

Amanda Taylor
Washington University School of Medicine in St. Louis

Michael Vasek
Washington University School of Medicine in St. Louis

See next page for additional authors

Cellular/Molecular

Diverse Voltage-Sensitive Dyes Modulate $GABA_A$ Receptor Function

Steven Mennerick,[1,2]* Mariangela Chisari,[1]* Hong-Jin Shu,[1] Amanda Taylor,[1] Michael Vasek,[4] Lawrence N. Eisenman,[3] and Charles F. Zorumski[1,2]

Departments of [1]Psychiatry, [2]Anatomy and Neurobiology and [3]Neurology, and [4]Graduate Program in Neuroscience, Washington University School of Medicine, St. Louis, Missouri 63110

Voltage-sensitive dyes are important tools for assessing network and single-cell excitability, but an untested premise in most cases is that the dyes do not interfere with the parameters (membrane potential, excitability) that they are designed to measure. We found that popular members of several different families of voltage-sensitive dyes modulate $GABA_A$ receptor with maximum efficacy and potency similar to clinically used $GABA_A$ receptor modulators. Di-4-ANEPPS and DiBAC4(3) potentiated GABA function with micromolar and high nanomolar potency, respectively, and yielded strong maximum effects similar to barbiturates and neurosteroids. Newer blue oxonols had biphasic effects on $GABA_A$ receptor function at nanomolar and micromolar concentrations, with maximum potentiation comparable to that of saturating benzodiazepine effects. ANNINE-6 and ANNINE-6plus had no detectable effect on $GABA_A$ receptor function. Even dyes with no activity on $GABA_A$ receptors at baseline induced photodynamic enhancement of $GABA_A$ receptors. The basal effects of dyes were sufficient to prolong IPSCs and to dampen network activity in multielectrode array recordings. Therefore, the dual effects of voltage-sensitive dyes on GABAergic inhibition require caution in dye use for studies of excitability and network activity.

Introduction

There has been a recent resurgence in the use of voltage-sensitive dyes (VSDs) as tools to probe single-cell and network activity in the CNS, as the photon comes to rival the electron in studies of neuronal function (Grinvald and Hildesheim, 2004; Stuart and Palmer, 2006; Scanziani and Häusser, 2009). A premise underlying their use is that the dyes do not directly or indirectly affect the parameter (i.e., membrane potential, neuronal activity) that they are designed to measure. This assumption has gone largely untested. Among many possible relevant targets of dyes, $GABA_A$ receptors represent a strong suspect. $GABA_A$ receptors are positively modulated by a wide variety of substances through specific binding sites. Compounds in this class include barbiturates, benzodiazepines, neurosteroids, ethanol, and many anesthetics. In addition, $GABA_A$ receptors are modulated, apparently nonselectively, by structurally diverse amphiphilic compounds (Søgaard et al., 2006; Yang and Sonner, 2008). Finally, GABA receptors are susceptible to photodynamic regulation (Chang et al., 2001; Leszkiewicz and Aizenman, 2003; Eisenman et al., 2007); therefore voltage-sensitive dyes could photosensitize modification of receptor function.

Because VSDs are inherently amphiphilic, we tested representatives of widely used voltage-sensitive dye families, the slow indicator oxonols and the fast indicator aminonaphthylethnylpyridinium (ANEP) dyes, in functional assays of GABA receptor activity. We also tested the newer dyes ANNINE-6 and ANNINE-6plus. We found that at relevant concentrations, representatives of oxonol and ANEP families have strong positive modulatory effects on $GABA_A$ receptors expressed in oocytes and native receptors in rat hippocampal neurons. Modulation was voltage independent and potency and efficacy comparable to neurosteroids and barbiturates. In addition to their basal effects on $GABA_A$ receptor function, VSDs have photodynamic effects on $GABA_A$ receptor function. Even compounds inactive at baseline exhibited photodynamic activity. In synaptic and in multielectrode array recordings of network activity in hippocampal cultures, we found that Di-4-ANEPPS, a commonly used fast indicator, directly gated currents, strongly prolonged IPSCs and reduced neuronal activity in the absence of light stimulation. Our results demonstrate that dual caution is warranted in the use of VSDs for studies of neuronal activity.

Materials and Methods

Hippocampal cultures. Primary cultures were prepared from postnatal day 0–3 rat pups as previously described (Shu et al., 2004). Rat pups were anesthetized with isoflurane and the hippocampus was cut into 500-μm-thick slices. The slices were digested with 1 mg/ml papain in oxygenated Leibovitz L-15 medium (Invitrogen) and mechanically triturated in modified Eagle's medium (Invitrogen) containing 5% horse serum, 5% fetal calf serum, 17 mM D-glucose, 400 μM glutamine, 50 U/ml penicillin, and 50 μg/ml streptomycin. Cells were plated in modified Eagle's medium at a density of ~650 cells/mm^2 on collagen-coated tissue culture dishes (Falcon). Cultures were maintained at 37°C in a humidified incubator with 5%CO_2/95% air. Glial proliferation was halted 3–4 d after plating with 6.7 μM cytosine arabinoside. At 4–5 d after plating, half the culture medium was replaced with Neurobasal medium plus B27 supplement (both from Invitrogen).

Received Nov. 12, 2009; revised Dec. 23, 2009; accepted Jan. 4, 2010.

This work was supported by National Institutes of Health Grants GM47969, MH77791, AA017413 (C.F.Z.), NS44041 (L.N.E.), and NS54174 (S.M.), and a gift from the Bantly Foundation. We thank Ann Benz for help in preparation of the cultures, and other lab members for critical discussion.

*S.M. and M.C. contributed equally to this work.

Correspondence should be addressed to Steven Mennerick, Department of Psychiatry, 660 South Euclid Avenue, Campus Box 8134, St. Louis, MO 63110. E-mail: menneris@psychiatry.wustl.edu.

DOI:10.1523/JNEUROSCI.5607-09.2010

 0270-6474/10/302871-09$15.00/0

Imaging. Images were obtained with a Nikon C1 confocal laser scanning microscope (see Fig. 7) or with a cooled CCD camera mounted to a Nikon TE2000 epifluorescence microscope (see Fig. 4). Quantification was performed using MetaMorph imaging software (Molecular Devices). Regions of interest near the plasma membrane were used to quantify fluorescence intensity.

Single-cell electrophysiology. Whole-cell recordings were performed on hippocampal neuron cultures 8–13 d following plating with an Axopatch 200B amplifier (Molecular Devices). Cells were transferred from culture medium to an extracellular recording solution containing the following (in mM): 138 NaCl, 4 KCl, 2 $CaCl_2$, 1 $MgCl_2$, 10 glucose, 10 HEPES, 0.001 2,3-dihydroxy-6-nitro-7-sulfonyl-benzo[f]quinoxaline (NBQX), and 0.01 D-2-amino-5-phosphonovalerate (D-APV) at pH 7.25. Patch pipettes were filled with an internal solution containing the following (in mM): 130 cesium methanesulfonate, 4 NaCl, 5 EGTA, 0.5 $CaCl_2$, and 10 HEPES at pH 7.25. For synaptic experiments, cesium methanesulfonate was replaced with potassium chloride, and with cesium chloride for photopotentiation experiments. When filled with solution, pipette tip resistance was 4–6 MΩ. Cells were clamped at −60 or −70 mV unless otherwise indicated. Access resistance was 8–20 MΩ and was not compensated for exogenous applications or for miniature IPSC recordings, where current amplitudes were small. For evoked autaptic IPSCs, access resistance was compensated 80–90%. A voltage pulse to 0 mV (1.2 ms) triggered a presynaptic action potential that elicited the IPSC (Mennerick et al., 1995). Drug applications were made with a multibarrel, gravity-flow local perfusion system. The estimated solution exchange times were 120 ± 14 ms (10–90% rise), measured by the change in junction currents at the tip of an open patch pipette. Whole-cell recordings were performed at room temperature.

Network recordings. Multielectrode arrays (MEAs) were coated with poly-D-lysine and laminin per the manufacturer's instructions and dispersed cultures were grown as described above. At day *in vitro* (DIV)7 and DIV10, one-third of the medium was removed and replaced with fresh Neurobasal supplemented with B27 and glutamine. Recordings were made with the MEA-60 recording system (MultiChannel Systems) with the headstage in an incubator set at 29°C and equilibrated with 5% CO_2 in room air with no additional humidity. The lower temperature was necessary because the electronics in the headstage generate ~7°C of excess heat. The MEA itself rests on a heating plate inside the headstage that was heated so the cultures were maintained at 37°C. To allow extended recordings in the dry incubator, cultures were covered with a semipermeable membrane that allows diffusion of oxygen and carbon dioxide but not water (Potter and DeMarse, 2001). Di-4-ANEPPS was added directly from stock solutions to the culture medium from a sister culture under sterile conditions. The medium in the MEA was replaced with the dye-containing medium and allowed to re-equilibrate for ~5 min before recording. Data were amplified ×1100 and sampled at 5 kHz. Spikes were detected by threshold crossing of high-pass filtered data. The threshold was set individually for each contact at 5 SDs above the average root mean squared noise level. Baseline data were recorded immediately before dye treatment, after which the medium was again replaced and a final dataset collected. All datasets were 2 h long. Activity was quantified using the array wide spike detection rate (ASDR) (Wagenaar et al., 2006), defined as the number of spikes detected in all contacts of the MEA during each second of recording. The average ASDR for each 2 h dataset was used as a summary measure of activity. Activity during dye exposure was compared with the average of the baseline and wash activity levels using a paired *t* test with $p < 0.05$ considered significant.

Oocyte expression studies. Stage V–VI oocytes from sexually mature female *Xenopus laevis* (Xenopus One) were harvested under 0.1% 3-aminobenzoic acid ethyl ester anesthesia, according to protocols approved by the Washington University Animal Studies Committee. The follicular layer was removed by shaking for 20 min at 37°C in collagenase (2 mg/ml) dissolved in calcium-free solution containing the following (in mM): 96 NaCl, 2 KCl, 1 $MgCl_2$, and 5 HEPES at pH 7.4. Capped mRNA, encoding rat $GABA_A$ receptor α1, β2, and γ2L subunits, was transcribed *in vitro* using the mMESSAGE mMachine kit (Ambion) from linearized pBluescript vectors containing receptor-coding regions. Subunit transcripts were injected in equal parts (20–40 ng of total RNA) 8–24 h following defolliculation. Oocytes were incubated up to 5 d at 18°C in ND96 medium containing the following (in mM): 96 NaCl, 1 KCl, 1 $MgCl_2$, 2 $CaCl_2$, and 10 HEPES at pH 7.4, supplemented with pyruvate (5 mM), penicillin (100 U/ml), streptomycin (100 μg/ml), and gentamycin (50 μg/ml).

Oocyte electrophysiology. Oocyes were voltage clamped at −70 mV with a two-electrode voltage-clamp amplifier (Warner Instruments) 2–5 d following RNA injection. The extracellular recording solution was unsupplemented ND96 medium. Intracellular recording pipettes contained 3 M KCl and had open-tip resistances of 1 MΩ. Drugs were applied from a common tip via a gravity-driven multibarrel delivery system. Drugs were coapplied with no preapplication period. Cells were voltage clamped at −70 mV for all experiments and the peak current was measured for quantification of current amplitudes.

Data analysis and statistical procedures. Data acquisition and analysis of single-cell electrophysiology from oocytes and hippocampal neurons were performed with pCLAMP 9.0 software (Molecular Devices), except for analysis of spontaneous miniature IPSCs, which was performed with MiniAnalysis (Synaptosoft). Data plotting and curve fitting were performed with SigmaPlot (Systat Software). Curve fitting was performed on potentiation values calculated as $(M - G)/G$, where M is the response in the presence of GABA plus modulator and G is the response to GABA alone. Empirical fits to concentration–response relationships were achieved using a least-squares minimization to the Hill equation: $B_{max}[X^h/(EC_{50}^h + X^h)]$, where B_{max} is the maximum potentiation, h is the Hill coefficient, EC_{50} is the concentration of modulator producing 50% of maximum potentiation, and X is the test modulator concentration. LogP calculations (logarithm of the octanol:water partition coefficient) were performed using an online calculator that simultaneously calculates logP estimates from nine independent algorithms (ALOGPS 2.1; http://www.vcclab.org/lab/alogps/). Multielectrode array data were analyzed and plotted using Igor Pro (Wavemetrics). Data are presented as mean ± SE. Statistical differences were determined using Student's two-tailed *t* test.

Drugs, chemicals, and other materials. Compounds were obtained from Sigma with the following exceptions: Di-4-ANEPPS, Di-8-ANEPPS, and DiSBAC4(3) were from Invitrogen; DiBAC4(5), DiSBAC2(3), DiSBAC2(5), Oxonol V, and Oxonol VI were from AnaSpec; blue oxonols (RH1691, RH1692, and RH1838) were from Optical Imaging; and ANNINE-6 and ANNINE-6plus were from Sensitive Dyes. Dyes were prepared as stock solutions in dimethylsulphoxide (DMSO). Final DMSO concentration was <0.1%. At double this concentration (0.2% DMSO), we observed a small inhibition of $GABA_A$ receptor currents (5 ± 2%, $p < 0.05$, $N = 8$) but never potentiation, so DMSO effects cannot explain VSD potentiation.

Results

In initial experiments to test whether voltage-sensitive membrane probes alter $GABA_A$ receptor function, we expressed a rat α1β2γ2L $GABA_A$ subunit combination in *Xenopus* oocytes and assessed modulation of GABA current amplitudes by simultaneous coapplication of the oxonol VSD DiBAC4(3). For reference, structures of the dyes used in this study are shown in supplemental Figures 1 and 2 (available at www.jneurosci.org as supplemental material). We found strong maximum potentiation (~15-fold) and an EC_{50} value of 0.36 μM under these conditions (Fig. 1*A*,*C*). Importantly, this modulation was observed in the concentration range of oxonol compounds used for imaging studies. As is observed for high concentrations of many allosteric modulators of $GABA_A$ receptors, 3 μM DiBAC4(3) activated small currents in the absence of GABA (Fig. 1*A*, inset) (63 ± 5% of the response to 2 μM GABA, $N = 4$ oocytes), indicating that DiBAC4(3) weakly gates the receptor in the absence of agonist in addition to positive modulation of receptor function in the presence of agonist.

DiBAC4(3) is a member of an oxonol family of older, slower VSDs and has a barbituric acid structure that could partly ac-

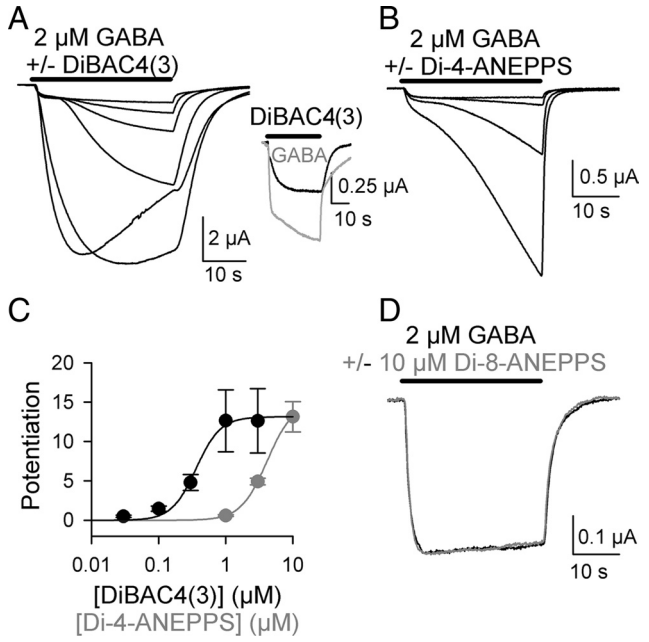

Figure 1. Members of two structurally distinct families of voltage-sensitive dyes strongly potentiate $GABA_A$ receptor currents in *Xenopus* oocytes expressing $\alpha1\beta2\gamma2L$ subunit combinations. ***A***, Representative traces of responses to GABA alone (2 μM) and to simultaneous coapplication of GABA with increasing concentrations (0.03–3 μM) of the oxonol dye DiBAC4(3). Horizontal bar above traces gives duration of exposure. The inset shows the response to 2 μM GABA alone (gray) and to 3 μM DiBAC4(3) alone (black). ***B***, Representative traces of another oocyte challenged with 2 μM GABA alone and GABA with simultaneously coapplied 1, 3, and 10 μM Di-4-ANEPPS. ***C***, Summary concentration–response relationships ($N = 4$ oocytes per data point). The solid lines are fits of the average data points to the Hill equation and yield an estimated EC_{50} for DiBAC4(3) of 0.36 μM. The estimated EC_{50} for Di-4-ANEPPS was 4.1 μM. ***D***, Another ANEP family member, Di-8-ANEPPS, failed to potentiate GABA currents.

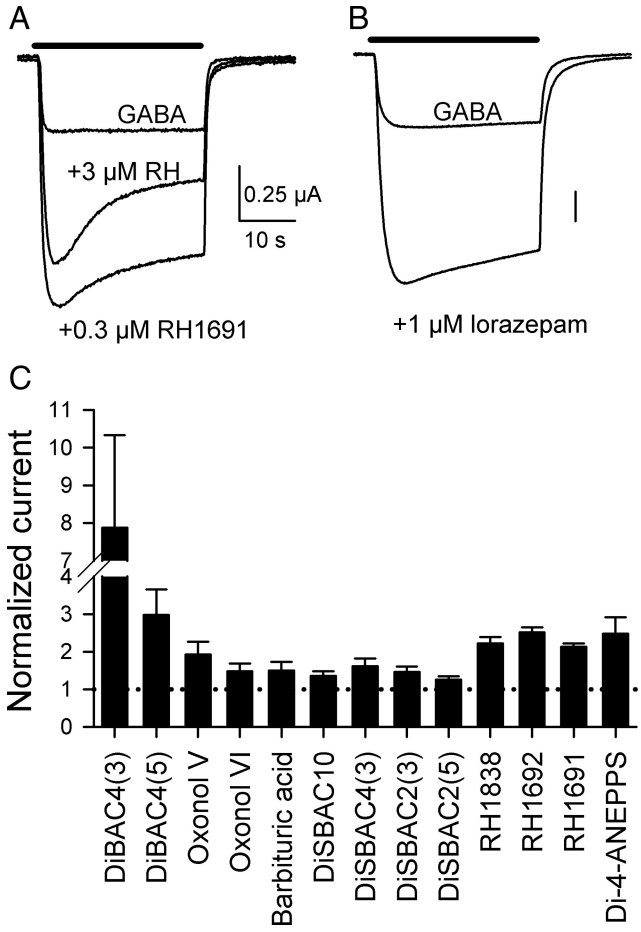

Figure 2. Potentiation by the oxonol family of dyes. ***A***, Biphasic potentiation of an oocyte GABA (2 μM) response by 0.3 and 3.0 μM RH1691, a blue oxonol dye. Note the stronger desensitization and blunted peak amplitude of the GABA response when coapplied with 3 μM RH1691 (RH) compared with the response to tenfold lower RH1691 concentration. ***B***, The potentiation by a saturating concentration (1 μM) of the benzodiazepine modulator lorazepam is shown for comparison on a different oocyte. Vertical bar is 250 nA. Time calibration same as in ***A***. ***C***, Summary of results from four to eight oocytes challenged with the indicated compounds at 0.3 μM. Compound structures are given in supplemental Figure 1 (available at www.jneurosci.org as supplemental material). The dotted line indicates the normalizing response to GABA alone. All compounds tested potentiated GABA responses significantly ($p < 0.05$) except for Oxonol VI and barbituric acid, which exhibited only trend level ($p < 0.08$) potentiation.

count for activity at $GABA_A$ receptors. We therefore tested Di-4-ANEPPS as a representative of a newer, faster VSD that enjoys widespread present usage (Iwasato et al., 2000; Tominaga et al., 2000; Airan et al., 2007; Maeda et al., 2007) and that is structurally different from the oxonols (supplemental Figs. 1 and 2, available at www.jneurosci.org as supplemental material). Di-4-ANEPPS also robustly modulated $GABA_A$ receptor currents when simultaneously coapplied with GABA (Fig. 1*B*,*C*). The concentration requirement was higher than that for DiBAC4(3), but concentrations were again in the range used in imaging studies ($EC_{50} = 4.1$ μM). Similar to DiBAC4(3), maximum potentiation was very strong (Fig. 1*B*,*C*), akin to that achieved by neurosteroids and barbiturates under similar conditions. No responses to agonist or to dyes were observed at the highest concentrations tested (3 and 10 μM for DiBAC4(3) and for Di-4-ANEPPS respectively) in control oocytes that were not injected with GABA receptor subunits, confirming that the currents observed indeed resulted from GABA receptor modulation ($N = 4$ oocytes, data not shown).

For neurosteroid actions at $GABA_A$ receptors, steroid lipophilicity plays a strong role in potency, at least for a range of structural steroid analogues (Chisari et al., 2009). To determine whether this rule applies to VSD modulation, we compared actions of Di-4-ANEPPS (calculated logP = 4.2 ± 0.3) with Di-8-ANEPPS (logP = 7.6 ± 0.3, see Materials and Methods). The higher logP of Di-8-ANEPPS results from a longer hydrophobic tail (supplemental Fig. 2, available at www.jneurosci.org as supplemental material). In contrast to neurosteroids, we found that the more hydrophobic Di-8-ANEPPS had no detectable effect on $GABA_A$ receptor function up to 10 μM (Fig. 1*D*). Currents in the presence of 10 μM Di-8-ANEPPS were 125 ± 13% of GABA currents in the absence of dye ($N = 12$ oocytes, $p > 0.05$). Therefore, the ANEP dye family also exhibits structural variability for $GABA_A$ receptor modulation, and results suggest that with care in choice of dye, basal GABA receptor effects may be avoided.

DiBAC4(3) also modulates certain BK potassium channel subunits, and this modulation has a specific structure-activity relationship (Morimoto et al., 2007). We exploited the structural diversity of the oxonol family, of which DiBAC4(3) is a member, to obtain structure-activity relationship data. We included in this screen three newer members of the oxonol family, so-called blue oxonols, which are rapid sensors of cellular activity (Shoham et al., 1999; Spors and Grinvald, 2002; Petersen et al., 2003). We found that each of the blue oxonols had a concentration-dependent biphasic effect on $GABA_A$ receptor function when evaluated at 0.3 μM and at 3 μM (Fig. 2*A*). The potentiation observed at 0.3 μM was similar to a saturating concentration of lorazepam (Fig. 2*B*) (lorazepam potentiation was 272 ± 13% of control, $N = 3$ oocytes). A summary of single-concentration (0.3

μM) screening is shown in Figure 2*C* and demonstrates variability among family members in their ability to modulate $GABA_A$ receptor function. We used a concentration that was near the EC_{50} for DiBAC4(3) so that we could detect stronger and weaker activity compared with DiBAC4(3). Interestingly, DiBAC4(3) was much stronger than any of the other family members at this subsaturating concentration (Fig. 2*C*). We raised the concentration of oxonol compounds in our screen tenfold, to 3 μM. Normalized current values did not increase dramatically for any of the oxonol compounds (range 0.97–3.61). Only the blue oxonols showed evidence of biphasic modulation (Fig. 2*A*). Overall, the failure of higher concentrations to increase potentiation suggests that the modest potentiation values reflect low efficacy of modulation rather than low potency. In general, the structure-activity relationship was distinct from that observed for BK channel subunits (Morimoto et al., 2007) (see Discussion).

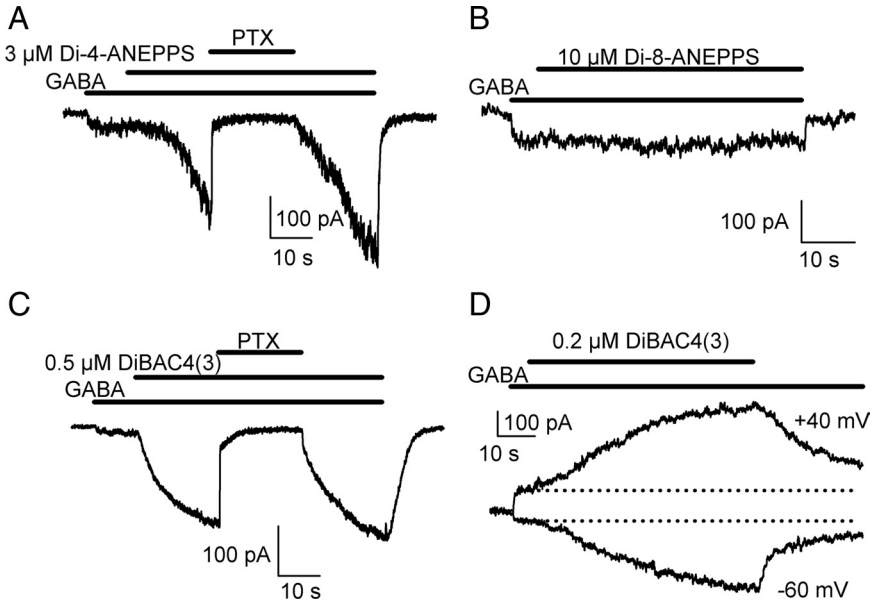

Figure 3. Dyes potentiate native receptors in hippocampal neurons. ***A***, DiBAC4(3) (0.5 μM) causes strong, picrotoxin-sensitive potentiation of the response to 0.5 μM GABA in a hippocampal neuron. Picrotoxin concentration was 100 μM. ***B***, The GABA (0.5 μM) response of another cell to 10 μM Di-8-ANEPPS was not potentiated. ***C***, The response of a neuron to 0.5 μM GABA plus 3 μM Di-4-ANEPPS. ***D***, The GABA modulatory effect of the VSDs was not strongly voltage dependent. Shown is a representative cell challenged with 0.5 μM GABA and 0.2 μM DiBAC4(3) at −60 mV and at +40 mV. Dotted lines denote the initial GABA response before addition of dye.

We also obtained limited quantities of the newer fast indicators ANNINE-6 and ANNINE-6plus dyes (Fromherz et al., 2008). When screened at 0.3 and at 3 μM against responses to 2 μM GABA, we failed to observe any significant potentiation of currents. GABA responses were in fact diminished slightly, but not in a clearly concentration-dependent manner (ANNINE-6: 89 ± 3% and 83 ± 2% depression at 0.3 and 3 μM respectively, $N = 3$ oocytes; ANNINE-6plus: 81 ± 3% and 80 ± 1% depression at 0.3 and 3 μM respectively).

In subsequent studies, we examined whether VSDs also modulate GABA receptors in mammalian cells. Based on results of the oocyte screening studies, we tested DiBAC4(3) and Di-4-ANEPPS as representative positive modulators and Oxonol VI and Di-8-ANEPPS as representative weak potentiators in cultured hippocampal neurons. Results paralleled those from oocytes. Again, at modest concentrations, both DiBAC4(3) (0.2–0.5 μM) and Di-4-ANEPPS (3–10 μM) profoundly potentiated responses to low GABA concentration (Fig. 3*A*,*C*), while neither 1 μM Oxonol VI (data not shown) nor 10 μM Di-8-ANEPPS (Fig. 3*B*) had any reliable potentiating effect in any cells tested ($N = 5$ and 3, respectively). Responses to DiBAC4(3) and to Di-4-ANEPPS in the presence of GABA were sensitive to application of 100 μM picrotoxin (Fig. 3*A*,*C*). Therefore, dye-induced potentiation clearly resulted from interaction of dyes with $GABA_A$ receptors.

Some VSDs, particularly slow indicators, indicate membrane potential in part by translocation within the membrane in response to changes in the transmembrane voltage (Waggoner and Grinvald, 1977; González and Tsien, 1995). This movement alters position of the environment-sensitive fluorophore and thus fluorescence, and allows use of these fluorophores in FRET studies. We wondered whether voltage-sensitive movement of the fluorophore might register as voltage-sensitive potentiation of GABA currents if intramembrane movement is important to access a VSD receptor site. However, neither DiBAC4(3) (Fig. 3*D*) nor Di-4-ANEPPS potentiation exhibited strong voltage dependence. Potentiation at −60 mV and at +40 mV was 173 ± 44% and 141 ± 29% respectively for DiBAC4(3) ($N = 4$ cells). For Di-4-ANEPPS potentiation was 437 ± 81% and 350 ± 30% at the two potentials (N = 8 cells). Furthermore, Di-8-ANEPPS, which was inert at −60 mV, was also inert at +40 mV (N = 3).

Di-8-ANEPPS could exhibit dramatically weaker effects on $GABA_A$ receptors than Di-4-ANEPPS because it fails to fulfill pharmacophore requirements for binding to a site on the $GABA_A$ receptor. Alternatively or additionally, Di-8-ANEPPS could fail to reach the binding site because its cellular accumulation and access to a putative GABA receptor site could differ from Di-4-ANEPPS. For instance, the rate of cellular accumulation of the two dyes has been reported to differ in cardiac cells (Rohr and Salzberg, 1994), and this could alter access to transmembrane or cytoplasmic targets on the receptor. As a simple test of whether slow accumulation could participate in the weak Di-8-ANEPPS activity on $GABA_A$ receptors, we examined responses of oocytes incubated for 10 min in the presence of 10 μM Di-8-ANEPPS. We observed only a minimal increase in Di-8-ANEPPS effect with long incubation. Currents after soaking were 23 ± 4% larger than those observed with acute Di-8-ANEPPS application ($N = 4$ oocytes).

To determine whether cellular retention patterns in hippocampal neurons differed between Di-4-ANEPPS and Di-8-ANEPPS, we imaged the time course of dye accumulation and maximum fluorescence in hippocampal neurons. We found that the two dyes differed dramatically in their cellular accumulation (Fig. 4). Di-4-ANEPPS exhibited bright fluorescence, initially restricted to the plasma membrane, but which over a course of minutes became strongly internalized within neurons (Fig. 4*A*). In contrast, 2 min of incubation in 10 μM Di-8-ANEPPS failed to produce cellular fluorescence levels comparable to Di-4-ANEPPS and did not produce fluorescence internalization (Fig. 4*A*,*B*). This pattern of comparatively weak fluorescence persisted with incubation times of up to 15 min. Di-4-ANEPPS perimembrane fluorescence at 15 min was >5-fold higher than Di-8-ANEPPS.

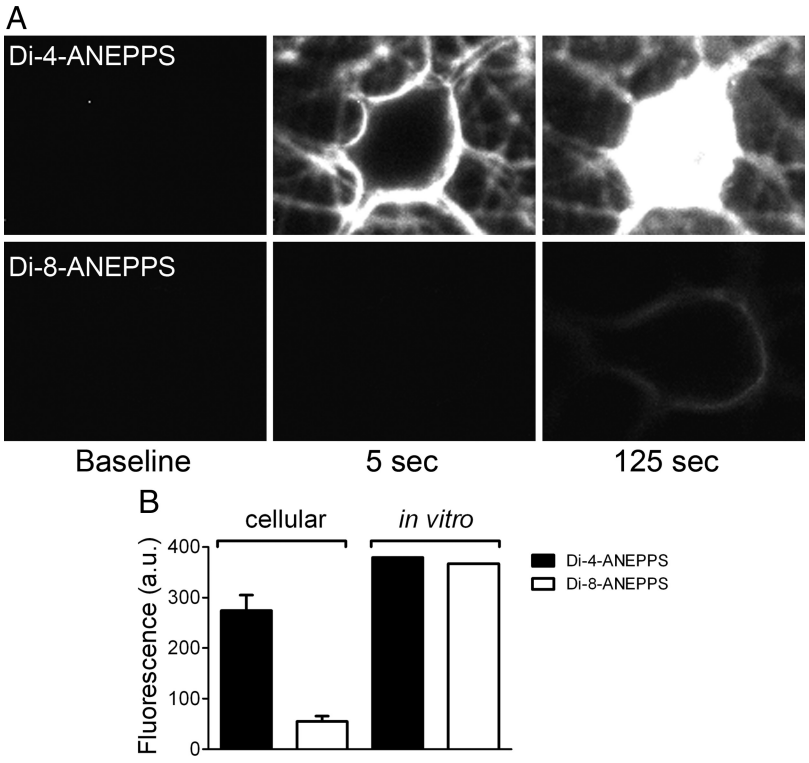

Figure 4. Differences in uptake of Di-4-ANEPPS and Di-8-ANEPPS correlate with $GABA_A$ receptor activity. ***A***, Fluorescence images of Di-4-ANEPPS and Di-8-ANEPPS (10 μM) perfused onto cultured hippocampal neurons. Images were acquired at the time points indicated below the figures. Acquisition and display gain settings were matched. ***B***, Summary of fluorescence for the two dyes. Left bars (cellular), Fluorescence was measured at 125 s of application time on three cells from different fields. A perimembrane region of interest was used to quantify fluorescence of both dyes. Right bars (*in vitro*), Cell-free fluorescence in propanol solvent for the two dyes.

The difference in maximum fluorescence of the dyes did not result from a difference in the inherent fluorescence of the two dyes because when dissolved in propanol at 50 μM and imaged in solution in the absence of cells, the dyes exhibited nearly identical fluorescence (Fig. 4*B*). In summary, we cannot exclude the possibility that cellular accumulation differences that result in differential access to the receptor might participate in the differences in $GABA_A$ receptor activity between the two tested ANEP dyes.

We recently showed that GABA receptors are subject to photodynamic effects in the presence of fluorophores that gain proximity to the GABA receptor, with fluorescent neurosteroid analogues serving as particularly potent photosensitizers (Eisenman et al., 2007). To test whether VSDs also elicit photodynamic positive modulation of GABA receptors, we challenged hippocampal neurons with excitation wavelengths in the presence of VSDs. To account for baseline activity of DiBAC4(3), we preincubated hippocampal neurons in a DiBAC4(3) concentration that produces little baseline potentiation (0.02 μM). Currents in response to 0.5 μM GABA were robustly potentiated by 480 nm light used to excite DiBAC4(3) fluorescence (Fig. 5*A*) (81 ± 11% potentiation at −60 mV in 4 cells tested). GABA responses are not sensitive to light stimulation alone at this wavelength (Eisenman et al., 2007). The photodynamic effect, like the baseline effect, was not detectably sensitive to voltage (Fig. 5*B*) (83 ± 26% potentiation, $N = 4$). We also tested Di-8-ANEPPS, a VSD with no baseline activity at $GABA_A$ receptors. At 10 μM, we confirmed that Di-8-ANEPPS had little or no baseline activity (Fig. 5*C*) (46 ± 17% potentiation, $N = 11$). However, upon 480 nm light excitation, GABA responses were potentiated 483 ± 168% ($N = 11$) over baseline GABA responses. ANNINE-6plus (3 μM) was also evaluated in the photopotentiation assay as another example of an inert dye (Fig. 5*D*). We found that cells treated with ANNINE-6plus were quite sensitive to phototoxicity, exhibiting large irrecoverable currents upon light stimulation; therefore we reduced light exposure to 12–25% of control (Fig. 5*D*) ($N = 3$) and to 3% of standard light level ($N = 1$), where we still observed robust photopotentiation. Our previous work has characterized the time course and other details of photopotentiation and has shown that photodynamic effects result in long-lived changes in $GABA_A$ receptor function (Eisenman et al., 2007; Shu et al., 2009). The present results suggest that VSDs can have dual potentiating effects on $GABA_A$ receptors; even compounds with no activity at baseline elicit photodynamic effects.

The actions of VSDs on $GABA_A$ receptor function suggest that, akin to barbiturates and other modulators, active compounds are likely to dampen network activity. However, our tests of receptor modulation used low concentrations of exogenous GABA, a situation rather far removed from endogenous signaling. It is therefore not clear whether VSDs would have important effects on network function in a situation where endogenous transmitters are involved. As a first step, we examined the effect of representative dyes, in the absence of light excitation, on GABA synaptic function. Figure 6, *A* and *B*, shows the effect of RH1691 (0.3 μM) and Di-4-ANEPPS (5 μM) on GABA-mediated evoked autaptic responses (IPSCs) from hippocampal neurons in culture. Di-4-ANEPPS elicited reversible increases in the holding current (−69 ± 30 pA, $N = 5$) that are not evident in Figure 6*B*, where baseline currents were subtracted. This likely resulted from direct activation of receptors in the absence of GABA. This change in holding current was not evident with 0.3 μM RH1691 (8 ± 7 pA, $N = 5$). The major change produced by both dyes on synaptic events was a prolongation of IPSCs (Fig. 6*A*,*B*), similar to that observed with other positive modulators of $GABA_A$ receptor activity (Hemmings et al., 2005). On average peak IPSCs were changed by −2 ± 8% and 28 ± 13% by 0.3 μM RH1691 and 5 μM Di-4-ANEPPS respectively. IPSC decays were prolonged by 32 ± 5% and by 173 ± 30% respectively ($p < 0.05$, $N = 5$ cells for both compounds).

The prolongation of IPSCs, with weak effects on peak amplitude, suggests a primarily postsynaptic locus of dye effect, with little effect on the presynaptic voltage-gated channels responsible for action potential propagation and Ca^{2+} influx. As a further test of a postsynaptic locus, we also examined effects of 3 μM Di-4-ANEPPS on spontaneous miniature IPSCs, recorded in the presence of 0.5 μM tetrodotoxin (Fig. 6*C*). Dye again produced a substantial change in holding current (data not shown) and increased membrane noise (Fig. 6*C1*,*C2*), consistent with direct gating of receptors by dye. Miniature IPSCs were prolonged by dye in a reversible manner (Fig. 6*C4*) (96 ± 20% increase in decay time, $N = 5$). In addition we observed a significant increase in peak amplitude of miniature IPSCs (50 ± 16% of control, $N = 5$

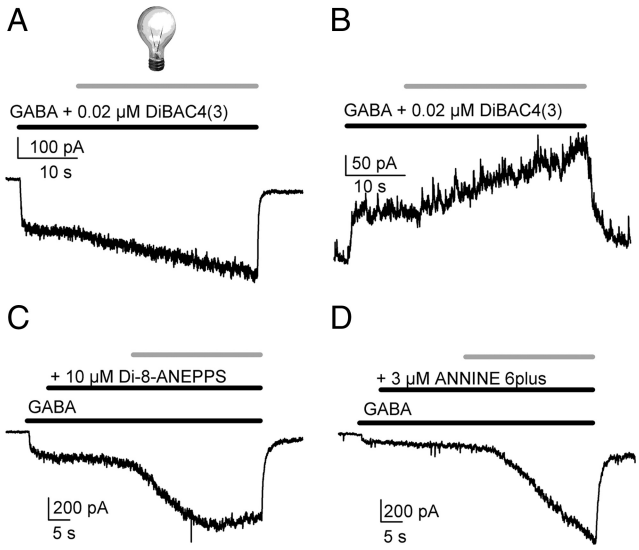

Figure 5. Photodynamic effects of dyes. ***A***, GABA (0.5 μM) and DiBAC4(3) (0.02 μM) were coapplied. At the time point denoted by the gray bar and light bulb, cells were epifluorescently illuminated with 480 nM light to excite fluorescence. ***B***, In another cell, the same protocol was performed at 40 mV. ***C***, ***D***, Di-8-ANEPPS (10 μM) and ANNINE-6plus (3 μM), representatives of basally inactive dyes, also exhibited photodynamic potentiation of receptor function. ANNINE-6plus exhibited notable phototoxicity in our cells. Therefore light intensity was reduced to 12% of standard for the experiment in ***D***.

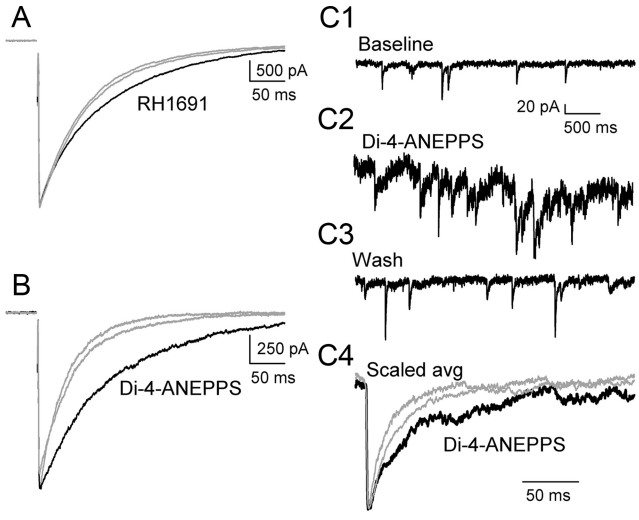

Figure 6. Effects of dyes on evoked IPSCs and spontaneous miniature IPSCs. ***A***, ***B***, Effects of RH1691 (0.3 μM) and Di-4-ANEPPS (5 μM) on autaptic-evoked IPSCs. Gray traces represent baseline and washout (90 s) traces. The black traces represent evoked IPSCs in the presence of the indicated dye (30–60 s preincubation before stimulation). Average baseline 10–90% decay time was 148.3 ± 43 ms ($N = 5$ cells). ***C***, Effect of Di-4-ANEPPS on miniature IPSC events. ***C1***–***C3***, Representative samples of spontaneous currents recorded in the presence of NBQX (1 μM), D-APV (25 μM), and tetrodotoxin (0.5 μM) in a cell from a mass culture. Not apparent is the increase in holding current evidence in ***C2***, associated with increased membrane noise. ***C4***, Average waveforms of aligned, scaled, miniature IPSCs from the three conditions shown in ***C1***–***C3***. Control and washout (gray) traces are averages of 31 and 107 events, respectively. The trace obtained in Di-4-ANEPPS represents 42 averaged events.

cells) and an apparent increase in frequency of miniature IPSCs (152 ± 58% of control). Based on the significant miniature IPSC frequency increase, we cannot exclude a presynaptic effect of dye, although this apparent change could in part result from increased membrane noise in the presence of dye, leading to an increase in detection of falsely positive synaptic events (Fig. 6*C*).

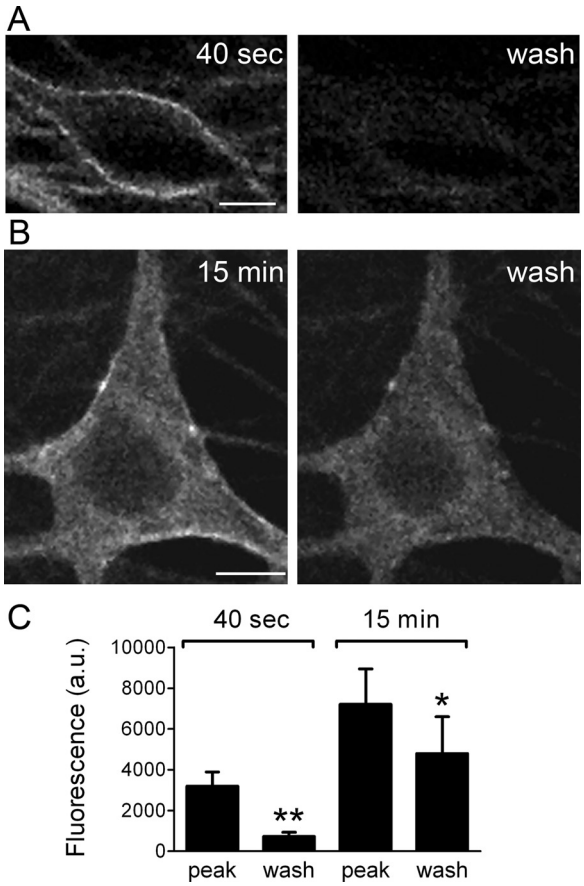

Figure 7. Reversibility of Di-4-ANEPPS effects matches reversibility of cellular accumulation following brief applications. ***A***, Example of cellular fluorescence of Di-4-ANEPPS during a 40 s wash-on, similar to that used in electrophysiology experiments, and after a 90 s washout. ***B***, In a different cell, 15 min of wash-on produced more intracellular fluorescence, and 90 s of washout did not return fluorescence to baseline. ***C***, Left bars, Summary of perimembrane fluorescence during the 40 s wash-on and 90 s wash-off from cells in five separate fields. Right bars, Summary of the perimembrane fluorescence after 15 min of incubation and after 90 s of washout ($N = 4$ cells).

It was clear that effects of Di-4-ANEPPS were largely reversible upon washout. This reversibility may be somewhat unexpected, since many experiments load cells or tissue with Di-4-ANEPPS, washout-free dye, and perform subsequent imaging of retained dye for many minutes (Yuste et al., 1997; Wachowiak and Cohen, 1999; Arata and Ito, 2004). To determine whether this reversibility was paralleled by cellular fluorescence, we imaged wash-on and washout of Di-4-ANEPPS (Fig. 7). Figure 7*A* shows that when applied for 40 s, Di-4-ANEPPS was localized mainly to the plasma membrane (Fig. 4*A*), and was largely reversible over the subsequent 90 s of wash (Fig. 7*A*,*C*). This is consistent with washout times observed in our electrophysiology studies. In contrast, with longer incubations of 15 min (Fig. 7*B*), dye was internalized, reached brighter fluorescence, and failed to readily reverse over a subsequent 90 s wash (Fig. 7*B*,*C*). Therefore, reversibility of GABA actions is expected of brief incubations, consistent with our electrophysiology protocols. Over longer incubations, the impact of cell internalization and slow washout times might be expected to influence effects.

To test the impact of longer dye incubation on synaptic function, we assessed the currents directly gated by Di-4-ANEPPS after prolonged incubations (15 min) in 10 μM Di-4-ANEPPS. Evaluation was performed on sibling cultures after vehicle con-

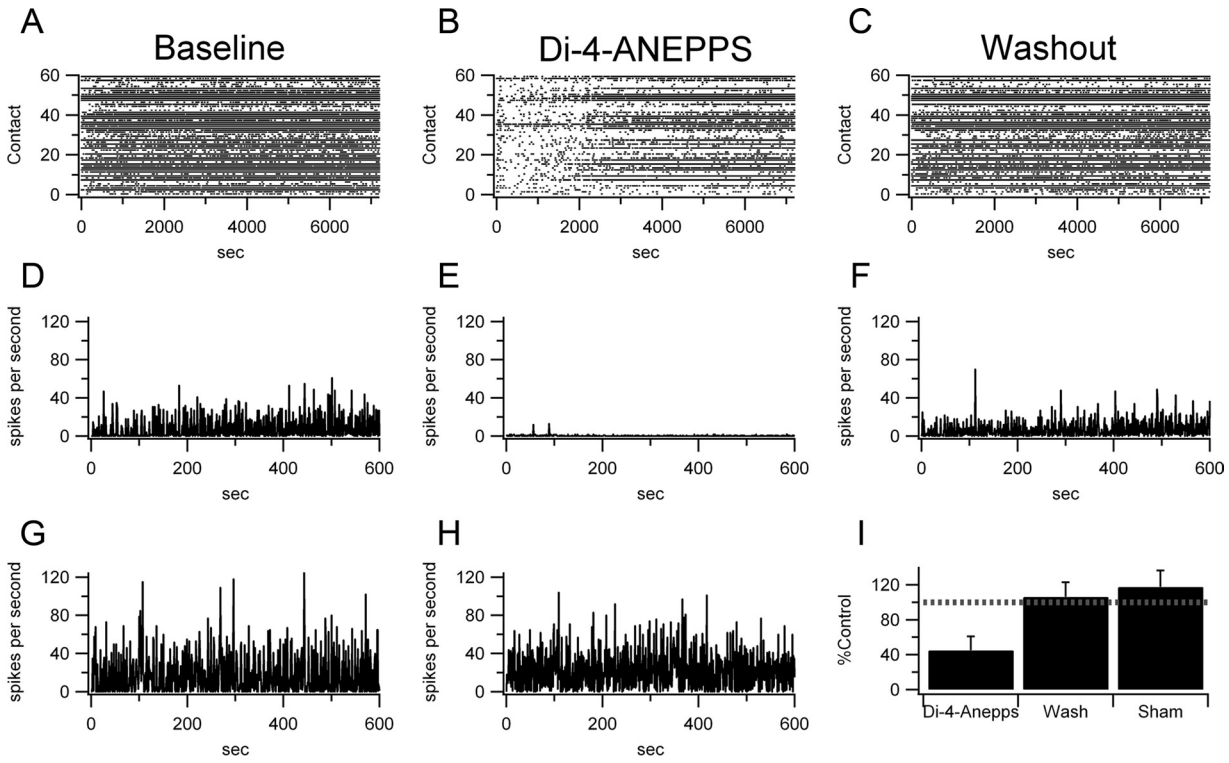

Figure 8. ***A–F***, Di-4-ANEPPS suppresses network activity of hippocampal cultures at a concentration typically used for voltage measurements. MEA recordings from a day *in vitro* 12 dissociated hippocampal culture showed robust basal activity (***A***) that was inhibited by 10 μM Di-4-ANEPPS but slowly rebounded during prolonged incubation (***B***). ***C***, Activity recovered on washout of free dye, likely through a combination of rebound and true washout. ***A–C*** are raster plots in which each vertical line represents a single spike and show the full 2 h recording period in each condition. ***D–F***, From the same culture represented in ***A–C***, the panels illustrate the number of spikes detected across the entire multielectrode array plotted as a function of time for the first 10 min of each condition in ***A–C***. ***G–H***, Similar array-wide spike rates from 10 min segments obtained from another culture subjected to control medium exchanges with no dye. ***I***, Summary of overall activity in the indicated conditions relative to baseline ($N = 4$ experiments for Di-4-ANEPPS and wash; $N = 7$ for sham).

trol incubation, in the continued presence of dye, or following free dye removal, to simulate the way Di-4-ANEPPS is often used in slice experiments (incubation followed by imaging in dye-free solutions). Glutamate blockers were present in all recording solutions, and cells were clamped at −70 mV using a CsCl-filled pipette. After prolonged dye exposure, we recorded from neurons and locally perfused 100 μM picrotoxin to evaluate the standing $GABA_A$ receptor-gated current under the various conditions. In control cells, there was a barely detectable picrotoxin-sensitive standing current (3.4 ± 1.0 pA, $N = 8$ cells). Prolonged incubation with recordings in the continued presence of dye yielded larger picrotoxin-sensitive currents (46.3 ± 9.7 pA, $N = 7$). After prolonged Di-4-ANEPPS incubation with recordings performed in the absence of dye, we recorded intermediate sized $GABA_A$ receptor currents (10.0 ± 1.4 pA, $N = 7$; $p < 0.01$ relative to control and relative to the persisting incubation condition). These results suggest that despite removal of free dye, some effects on GABA receptors linger as a result of retained dye, although these effects are not as strong as the acute dye effects.

To test directly the impact of VSD actions at GABA receptors on network activity, we examined the effects of Di-4-ANEPPS on network spiking activity recorded in dissociated hippocampal cultures plated on multielectrode arrays. Overall spontaneous activity in the cultures was strongly inhibited when the medium was switched to medium containing 10 μM Di-4-ANEPPS (Fig. 8). Note that no light stimulation of the fluorophore was used in these studies. Cells were maintained in a dark incubator for the measurements, so results represent basal, rather than photodynamic, effects of Di-4-ANEPPS. In four experiments, the average spike activity during a 2 h incubation in dye decreased to 45 ± 16% of control levels (Fig. 8*I*). Inhibition was clearly biased toward the early period of dye exposure (Fig. 8*B*). In the first 10 min, activity was nearly abolished compared with the final 10 min of control (Fig. 8, *E* vs *D*), but spiking strongly rebounded in the continued presence of dye (Fig. 8*B*). The inhibition of activity did not result from the medium exchange alone, as medium exchange produced no significant change in activity (activity was 118 ± 19% of baseline in the 10 min following medium exchange, $p = 0.39$; $N = 7$ cultures) (Fig. 8*G–I*). In dye-treated cultures suppression of activity recovered to 106 ± 17% following washout of free dye (Fig. 8*I*) ($p < 0.05$). Given the rebound of activity during prolonged dye incubation and because of strong retention of dye following prolonged incubation (Fig. 7*B*,*C*), it seems likely that the recovery after washout of free dye represents the combination of true washout and the rebound phenomenon. Regardless, our main result is that Di-4-ANEPPS acutely and strongly reduced neuronal activity, the parameter the dye is meant to measure.

Discussion

We show strong, positive modulation of $GABA_A$ receptors by several structurally diverse VSDs at concentrations relevant to their use as voltage indicators. Effects of several VSDs are similar to neurosteroids and to barbiturates, with 15–20-fold maximum potentiation at low GABA concentrations. DiBAC4(3) has potency similar to neurosteroids and much greater than barbiturates. Di-4-ANEPPS exhibits potency comparable to or greater than barbiturates. Although drawbacks of VSDs have been noted

before (Stuart and Palmer, 2006), interaction of these dyes with $GABA_A$ receptors is particularly problematic because of the ubiquity of this receptor class in virtually all neurons, the strong potency and efficacy of potentiation, direct dye activation of the receptor even in the absence of agonist, and the dual light-independent and light-dependent components of potentiation.

Our analysis gives some clues about structural attributes that may be important for oxonol and ANEP dye potentiation. Oxonols exhibited a distinct structure activity relationship for $GABA_A$ receptors compared with that reported for modulation of certain BK channel subunits (Morimoto et al., 2007). Specifically, BK channel effects tolerated a thiobarbituric acid structure (Morimoto et al., 2007), but thiol addition was not well tolerated for GABA receptor interactions. For GABA receptors, the barbiturate ring structure may be important for potentiation since a single barbituric acid yielded weak potentiation. However, it is also clear that either increasing or decreasing the length of the oligomethine chain reduced activity at the receptors. Similarly for the ANEP dyes, a longer hydrophobic tail (Di-8-ANEPPS) reduced activity at $GABA_A$ receptors. Unfortunately, these observations do not yield sufficiently strong conclusions to offer predictions for other dyes.

Structure-activity relationships may be particularly intractable if dyes access a transmembrane binding site via the lipid phase, similar to neurosteroids (Akk et al., 2005; Chisari et al., 2009). In this case, structural features affecting the ligand's interaction with the membrane could affect its ability to access the receptor site, in addition to any true pharmacophore effects (Makriyannis et al., 2005; Chisari et al., 2009). Low concentrations of DiBAC4(3) and Di-4-ANEPPS exhibited very slow onset kinetics relative to GABA in both oocytes (Fig. 1) and hippocampal neurons (Fig. 2). Similarly slow kinetics are also hallmarks of neurosteroid actions (Shu et al., 2004) and could indicate that a process not limited by aqueous diffusion, such as membrane partitioning or permeation, contributes to binding-site access (Akk et al., 2005; Chisari et al., 2009). Complicating matters further is our observation that blue oxonols exhibit evidence for a biphasic effect on GABA receptor function, with mixed potentiation and inhibition at 3 μM (Fig. 2*A*). Pending a full understanding of the number of distinct sites involved in VSD modulation of $GABA_A$ receptors and how the VSDs access these sites, investigators will have to evaluate potential confounding effects of GABA receptor interactions on a case-by-case basis.

We also found that at least for our test compound Di-4-ANEPPS, length of incubation affected the compartmentalization of dye (Fig. 7), the ability to effectively remove cellularly retained dye (Fig. 7), and the effects on neuronal network activity (Fig. 8). The basis for the rebound of activity during prolonged Di-4-ANEPPS incubation is unclear. However, the rebound could be associated with the internalization of dye observed in Figure 7 with prolonged incubation. Alternatively, because we observed that directly gated picrotoxin-sensitive currents persisted with prolonged dye incubation, it is possible that the rebound in network activity was associated with compensatory synaptic or excitability changes.

Fluorescent dyes photodynamically modulate voltage-gated channels (Oxford et al., 1977; Duprat et al., 1995; Antic et al., 1999), giving rise to well known effects on action potential shape (Antic et al., 1999). These effects, like photodynamic effects on $GABA_A$ receptors, can be minimized by limiting light exposure. However, because of selective proximity gained by some VSDs to the GABA receptor by binding in the absence of light stimulation, photodynamic effects on $GABA_A$ receptors may be evident at light levels below those that elicit effects on other ion channels. For instance, fluorescent neurosteroid analogues that bind the $GABA_A$ receptor exhibit more potent photodynamic $GABA_A$ effects than analogues that do not bind the receptor (Eisenman et al., 2007; Shu et al., 2009). For reasons that are unclear, ANNINE-6plus, a dye that proved inert at baseline, was particularly efficient at generating photodynamic effects on $GABA_A$ receptor function in our experiments (Fig. 5*D*).

The light-independent effects of dyes described here are more difficult to circumvent. Similar to recently reported effects on membrane capacitance of protein voltage indicators (Akemann et al., 2009), the effects reported here on $GABA_A$ receptors are likely to be ubiquitous. Virtually all neurons express $GABA_A$ receptors, and we found that all hippocampal neurons tested were sensitive to $GABA_A$ modulation by oxonol and by Di-4-ANEPPS. Furthermore, 10 μM Di-4-ANEPPS significantly depressed network activity. Several of the oxonol compounds had weaker effects on GABA receptors than either DiBAC4(3) or Di-4-ANEPPS. However, use of these compounds is risky because the efficacy of these compounds approached that of benzodiazepines, another class of high potency, weak efficacy potentiators. Because benzodiazepines have well described effects on neuronal activity and excitability, it seems likely that weak oxonols will have similar effects. Clearly, careful dye choice is critical to avoid inadvertent VSD effects on the GABA system and neuronal excitability.

In summary, we have demonstrated dual light-independent and light-dependent actions of voltage-sensitive dyes on $GABA_A$ receptor function. These effects are of particular concern because of the ubiquity of GABA signaling throughout the nervous system and the importance of GABA to cellular and network excitability. Our results suggest caution in choice of dye and in experimental design to avoid inadvertent interference with neuronal activity.

References

Airan RD, Meltzer LA, Roy M, Gong Y, Chen H, Deisseroth K (2007) High-speed imaging reveals neurophysiological links to behavior in an animal model of depression. Science 317:819–823.

Akemann W, Lundby A, Mutoh H, Knöpfel T (2009) Effect of voltage sensitive fluorescent proteins on neuronal excitability. Biophys J 96:3959–3976.

Akk G, Shu HJ, Wang C, Steinbach JH, Zorumski CF, Covey DF, Mennerick S (2005) Neurosteroid access to the $GABA_A$ receptor. J Neurosci 25:11605–11613.

Antic S, Major G, Zecevic D (1999) Fast optical recordings of membrane potential changes from dendrites of pyramidal neurons. J Neurophysiol 82:1615–1621.

Arata A, Ito M (2004) Purkinje cell functions in the in vitro cerebellum isolated from neonatal rats in a block with the pons and medulla. Neurosci Res 50:361–367.

Chang Y, Xie Y, Weiss DS (2001) Positive allosteric modulation by ultraviolet irradiation on $GABA_A$, but not $GABA_C$, receptors expressed in *Xenopus* oocytes. J Physiol 536:471–478.

Chisari M, Eisenman LN, Krishnan K, Bandyopadhyaya AK, Wang C, Taylor A, Benz A, Covey DF, Zorumski CF, Mennerick S (2009) The influence of neuroactive steroid lipophilicity on $GABA_A$ receptor modulation: evidence for a low affinity interaction. J Neurophysiol 102:1254–1264.

Duprat F, Guillemare E, Romey G, Fink M, Lesage F, Lazdunski M, Honore E (1995) Susceptibility of cloned K^+ channels to reactive oxygen species. Proc Natl Acad Sci U S A 92:11796–11800.

Eisenman LN, Shu HJ, Akk G, Wang C, Manion BD, Kress GJ, Evers AS, Steinbach JH, Covey DF, Zorumski CF, Mennerick S (2007) Anticonvulsant and anesthetic effects of a fluorescent neurosteroid analog activated by visible light. Nat Neurosci 10:523–530.

Fromherz P, Hübener G, Kuhn B, Hinner MJ (2008) ANNINE-6plus, a

voltage-sensitive dye with good solubility, strong membrane binding and high sensitivity. Eur Biophys J 37:509–514.

González JE, Tsien RY (1995) Voltage sensing by fluorescence resonance energy transfer in single cells. Biophys J 69:1272–1280.

Grinvald A, Hildesheim R (2004) VSDI: a new era in functional imaging of cortical dynamics. Nat Rev Neurosci 5:874–885.

Hemmings HC Jr, Akabas MH, Goldstein PA, Trudell JR, Orser BA, Harrison NL (2005) Emerging molecular mechanisms of general anesthetic action. Trends Pharmacol Sci 26:503–510.

Iwasato T, Datwani A, Wolf AM, Nishiyama H, Taguchi Y, Tonegawa S, Knöpfel T, Erzurumlu RS, Itohara S (2000) Cortex-restricted disruption of NMDAR1 impairs neuronal patterns in the barrel cortex. Nature 406:726–731.

Leszkiewicz DN, Aizenman E (2003) Reversible modulation of $GABA_A$ receptor-mediated currents by light is dependent on the redox state of the receptor. Eur J Neurosci 17:2077–2083.

Maeda H, Ohno T, Sakurai M (2007) Optical and electrophysiological recordings of corticospinal synaptic activity and its developmental change in *in vitro* rat slice co-cultures. Neuroscience 150:829–840.

Makriyannis A, Tian X, Guo J (2005) How lipophilic cannabinergic ligands reach their receptor sites. Prostaglandins Other Lipid Mediat 77:210–218.

Mennerick S, Que J, Benz A, Zorumski CF (1995) Passive and synaptic properties of neurons grown in microcultures and in mass cultures. J Neurophysiol 73:320–332.

Morimoto T, Sakamoto K, Sade H, Ohya S, Muraki K, Imaizumi Y (2007) Voltage-sensitive oxonol dyes are novel large-conductance Ca^{2+}-activated K^+ channel activators selective for beta1 and beta4 but not for beta2 subunits. Mol Pharmacol 71:1075–1088.

Oxford GS, Pooler JP, Narahashi T (1977) Internal and external application of photodynamic sensitizers on squid giant axons. J Membr Biol 36:159–173.

Petersen CC, Grinvald A, Sakmann B (2003) Spatiotemporal dynamics of sensory responses in layer 2/3 of rat barrel cortex measured in vivo by voltage-sensitive dye imaging combined with whole-cell voltage recordings and neuron reconstructions. J Neurosci 23:1298–1309.

Potter SM, DeMarse TB (2001) A new approach to neural cell culture for long-term studies. J Neurosci Methods 110:17–24.

Rohr S, Salzberg BM (1994) Multiple site optical recording of transmembrane voltage (MSORTV) in patterned growth heart cell cultures: assessing electrical behavior, with microsecond resolution, on a cellular and subcellular scale. Biophys J 67:1301–1315.

Scanziani M, Häusser M (2009) Electrophysiology in the age of light. Nature 461:930–939.

Shoham D, Glaser DE, Arieli A, Kenet T, Wijnbergen C, Toledo Y, Hildesheim R, Grinvald A (1999) Imaging cortical dynamics at high spatial and temporal resolution with novel blue voltage-sensitive dyes. Neuron 24:791–802.

Shu HJ, Eisenman LN, Jinadasa D, Covey DF, Zorumski CF, Mennerick S (2004) Slow actions of neuroactive steroids at $GABA_A$ receptors. J Neurosci 24:6667–6675.

Shu HJ, Eisenman LN, Wang C, Bandyopadhyaya AK, Krishnan K, Taylor A, Benz AM, Manion B, Evers AS, Covey DF, Zorumski CF, Mennerick S (2009) Photodynamic effects of steroid conjugated fluorophores on $GABA_A$ receptors. Mol Pharmacol 67:754–765.

Søgaard R, Werge TM, Bertelsen C, Lundbye C, Madsen KL, Nielsen CH, Lundbaek JA (2006) $GABA_A$ receptor function is regulated by lipid bilayer elasticity. Biochemistry 45:13118–13129.

Spors H, Grinvald A (2002) Spatio-temporal dynamics of odor representations in the mammalian olfactory bulb. Neuron 34:301–315.

Stuart GJ, Palmer LM (2006) Imaging membrane potential in dendrites and axons of single neurons. Pflugers Arch 453:403–410.

Tominaga T, Tominaga Y, Yamada H, Matsumoto G, Ichikawa M (2000) Quantification of optical signals with electrophysiological signals in neural activities of Di-4-ANEPPS stained rat hippocampal slices. J Neurosci Methods 102:11–23.

Wachowiak M, Cohen LB (1999) Presynaptic inhibition of primary olfactory afferents mediated by different mechanisms in lobster and turtle. J Neurosci 19:8808–8817.

Wagenaar DA, Pine J, Potter SM (2006) An extremely rich repertoire of bursting patterns during the development of cortical cultures. BMC Neurosci 7:11.

Waggoner AS, Grinvald A (1977) Mechanisms of rapid optical changes of potential sensitive dyes. Ann N Y Acad Sci 303:217–241.

Yang L, Sonner JM (2008) Anesthetic-like modulation of receptor function by surfactants: a test of the interfacial theory of anesthesia. Anesth Analg 107:868–874.

Yuste R, Tank DW, Kleinfeld D (1997) Functional study of the rat cortical microcircuitry with voltage-sensitive dye imaging of neocortical slices. Cereb Cortex 7:546–558.